# Application of Downscaled Extreme Precipitation to Flood Control Agency Operations: A Framework for Stakeholder-driven Climate Science

**E. J. Dennis[1], N. Goldenson[1,2], W. Krantz[1], S. Rahimi[1], A. Hall[1], Iraj Nasseri[3]**

[1] Center for Climate Science, University of California, Los Angeles

[2] Model World Consulting LLC, Seattle, Washington

[3] Los Angeles County Flood Control District, Department of Public Works, California

Corresponding author: Eli Dennis (elidennis@g.ucla.edu)

†Additional author notes should be indicated with symbols (current addresses, for example)

**Key Points:**

- Extreme precipitation will increase in a warming world
- Dynamically-downscaled climate projections of increasing precipitation can be used to adapt urban flooding operations
- Highlights the importance of stakeholder engagement to enact positive change towards sustainability

## Abstract

Extreme precipitation is expected to intensify as the climate warms, but the magnitude of the increase will vary regionally. In many cases, global climate models (GCMs) are not well-suited to project the changes in extreme precipitation due to their coarse resolution, particularly over complex terrain. Here, we analyze an unprecedented suite of eight bias-corrected dynamically downscaled GCMs over the western U.S., which allow us to assess extreme precipitation changes at high resolution. We pool data across the downscaled ensemble to adequately sample extreme events and characterize 99.99th percentile precipitation in Los Angeles County, home to 10M people. This high-resolution data allows us to advise a county government agency on expected changes in local extreme precipitation so that they may consider the suitability of their urban design standards in the coming decades. We find that the 99.99th percentile precipitation event is expected to increase by about 6.5% per degree Celsius global warming on average over Los Angeles County. However, Los Angeles County contains numerous micro-climates associated with, e.g., high mountains, marine ecosystems, and urban centers, whose future changes the downscaled projections are uniquely suited to predict. The absolute increases in extreme precipitation are shown to be magnified in the mountains and minimized in the desert regions. The agency will use this data to become more resilient to climate change. This project underscores the importance of stakeholder engagement with scientists for translating climate data into actionable guidance.



## Plain Language Summary

Extreme precipitation is expected to increase globally but with uncertain regional variability. Due to their coarse resolution, global climate models (GCMs) are not proficient at describing future changes in regional extreme precipitation. To overcome the coarse resolution of GCMs, they need to be downscaled to a scale that captures regional climate. Our group has produced a large array of downscaled GCMs so that now we can describe the regional characteristics of changing extreme precipitation. We utilize these downscaled GCMs to advise a government agency on changes in county-scale extreme precipitation so that they may update their infrastructure and operations to become more resilient. We have found that the 99.99th percentile precipitation event (i.e., an event that occurs about once every 50 years) will increase

by about 6.5% per degree Celsius global warming on average in Los Angeles County. However, those increases vary in different parts of the county. The absolute increases in extreme precipitation are enhanced in the mountains and lessened in the deserts. The local agency plans to use this data to become more resilient to climate change. This project highlights the importance of stakeholder engagement with scientists for translating climate data into actionable guidance.

This is optional but will help expand the reach of your paper. Information on writing a good plain-language summary is available here.

# Introduction:

Climate change presents a significant threat to large-scale public works designed under assumptions of historical climate conditions. Yet, adaptation is challenging because practitioners and policymakers typically do not confront the deep uncertainty characteristic of the climate system (Wasko et al., 2021). Moreover, climate science should inform risk assessment and the planning process from inception to fruition (Sutton, 2019). Adapting to climate change requires flexible design and planning approaches (Wasko et al., 2021) and a willingness to update traditional methods to be more relevant in a changing climate. Therefore, climate change adaptation requires cooperation among scientists, practitioners, and policymakers. In this way, applied climate science targets can be produced through appropriate stakeholder engagement, communication, and adequate assessment of uncertainty to fit users' needs.

Anthropogenic greenhouse gas emissions have caused the Earth to warm by about 1ºC since the late 1800s. One expected consequence is the magnification of global precipitation intensity because of greater moisture availability in a warming atmosphere. Extreme precipitation is thought to increase at a rate consistent with the Clausius-Clapeyron (CC) theory (~7% $ºC^{-1}$ global warming; Trenberth, 2011). However, this is a general statement about the entire planet, and in some regions, it may intensify at a greater or lesser rate than CC predicts (especially sub-daily extremes; Moustakis et al., 2021; Westra et al., 2013). Moderate precipitation is expected to intensify at a lower rate or even decrease (Pendergrass, 2018), again with regional variations. The intensification of extremes has been detected in large areas (Fischer & Knutti, 2015; Min et al., 2011) and with a global signature (Madakumbura et al., 2021) and is expected to continue through the 21st Century (Alexander et al., 2006; O'Gorman, 2015; Westra et al., 2013). The United States specifically has seen an increase in extreme-precipitation magnitude (Kirchmeier-Young & Zhang, 2020) and frequency (Monier & Gao, 2015). Similarly, to the rest of the globe, these increases are expected to continue (Kunkel, 2003).

The western United States has seen a marked change in hydroclimate, with 60% of the changes occurring between 1950 and 1999 being human-induced (Barnett et al., 2008). In California, while mean precipitation is not expected to change greatly, the frequencies of both wet and dry extremes are expected to increase (Berg & Hall, 2015; Swain et al., 2018). The volume of the most extreme precipitation is expected to rise due to increases in both intensity and storm area

(Chen et al., 2023) Most extreme precipitation events in California are caused by atmospheric rivers (ARs; Dettinger, 2011; Hall et al., 2018; Harris & Carvalho, 2018). ARs are narrow corridors of intense atmospheric moisture transport. When ARs collide with topography, the moist air is lifted to create intense precipitation. ARs can cause severe flooding (Ralph et al., 2006) and significant economic losses (Corringham et al., 2022). However, they can also mediate long-term deficits in water resources (Dettinger, 2013). Because ARs make up almost all of California's extreme precipitation, governments throughout the state have a vested interest in understanding their evolution and the evolution of the associated extreme precipitation in a warming climate (Mailhot & Duchesne, 2010).

Flooding is a major concern, given California's projected increases in extreme precipitation (Das et al., 2011, 2013; Huang & Swain, 2022) Not all heavy rain results in pluvial flooding, however. In some cases, the antecedent soil moisture is so low that significant rainfall infiltrates the soil and replenishes water-stressed plants before accumulating downhill(Bass et al., 2023; Sharma et al., 2018; Wasko & Nathan, 2019). In dry periods the snowpack is also reduced, leading to reductions in the seasonal melt, creating even drier soils(Sharma et al., 2018). Furthermore, land-use and land-cover change can modulate flood intensity. Compared to unaltered and somewhat altered basins, urbanized basins have shown a higher percentage increase in peak streamflow (Hodgkins et al., 2019). Furthermore, in Los Angeles, inequitable flood risk has been reported to affect historically black and brown communities to a greater extent than historically white communities (Sanders et al., 2022). To protect against flooding, infrastructure has been developed based on risk standards to cope with certain rainfall magnitudes, defined using Intensity-Duration-Frequency (IDF) curves.

Based on a time series of annual maximum precipitation, IDF curves display a relationship between intensity and duration in frequency space (i.e., return period). While IDF curves are useful for connecting precipitation amounts to a likelihood of occurrence, they have some limitations. For instance, one of the major challenges is providing a precipitation record of sufficient length (K. Arnbjerg-Nielsen et al., 2013). Often rain gauges are used to estimate local recurrence intervals, and while some have long historical records, the minimum record length for a gauge to be included can be as short as 30 years. This minimum length would present a challenge if estimating the 99.99th percentile storm (roughly the 50-year storm) in Southern California—the standard reference for stormwater engineers in Los Angeles County.

Furthermore, standard IDF curves suffer from stationarity assumptions. Because IDF curves reflect the historical statistics, they do not reflect changing statistics brought about by climate change. Cheng and AghaKouchak (2014) showed that IDF curves would underestimate future extreme precipitation by up to 60% unless they were updated. Arnbjerg-Nielsen (2012) showed that precipitation, as defined by IDF curves, would increase by 10–60% in Denmark, but the rate of increase depends on the return period and storm duration. Arnbjerg-Nielsen et al. (2013) provide an extensive review of IDF curve-based urban drainage systems in the face of increasing extreme precipitation with climate change. They suggest that further study is necessary to understand climate change's effect on extreme precipitation locally and on the ability of urban drainage systems to cope with those changes.

Numerous studies have endeavored to update IDF curves to be more climate-aware (Cheng & AghaKouchak, 2014; Cook et al., 2017; Fadhel et al., 2017; Martel et al., 2021; Ragno et al., 2018; Srivastav et al., 2014; Yan et al., 2021; Yilmaz et al., 2014). According to a review, most mechanisms for updating IDF curves are either covariate-based nonstationary methods or GCM-based approaches, but both have limitations (Yan et al., 2021). For instance, there is a tradeoff between uncertainty and model complexity for covariate-based nonstationary models. Meanwhile, GCM-based estimates strongly depend on projections of future local climate, which are computationally expensive and come with their own uncertainty (Yan et al., 2021). Despite the complexity of updating IDF curves, it is a necessary practice for societal adaptation to climate change, given the intensification of short-duration rainfall extremes and the associated flooding (Fowler et al., 2021).

While updating IDF curves is challenging for the above reasons, implementing those updates in planning for infrastructure and operations is another obstacle. It requires communicating those updates clearly to stakeholders, which is challenging due to the deep uncertainty associated with climate projections. However, mechanisms can be utilized to make the communication of climate projections in a more digestible way. For example, employing the "storyline" approach allows for the translation of climate science to scenarios that are more relatable to practitioners (Shepherd et al., 2018). Additionally, using a "degree-warming framework" can remove the uncertainty of emissions scenario choices and, instead, frame the changes in the local environment as those that would accompany, for instance, a world that has warmed 2ºC since a pre-industrial mean. Finally, while there are many mechanisms for including the effects of

156 climate change in extreme precipitation, choosing one that is easily understood (i.e., not a black
157 box) and easily implemented into existing operations is critical for creating actionable change.
158 The adaptation must fit seamlessly into existing operational structures to allow for easy adoption.

159

160 With all the above considerations in mind, this study seeks to understand the evolution of a 50-
161 year, 24-hour storm (i.e., a particular magnitude storm from an IDF curve) in Los Angeles
162 County. The 50-year 24-hour storm (in $day^{-1}$) is the linchpin that guides flood control operations
163 in this area. The goals of this study have been established in close coordination with engineers
164 from the Los Angeles County Flood Control District (LACFCD). Using numerous carefully
165 selected, dynamically downscaled GCMs over the western U.S. (Rahimi et al. *under review*,
166 Krantz et al. *under review*), we provide a quantitative estimate of shifts in extreme precipitation
167 with climate change over Los Angeles County. This guidance is designed to be actionable for
168 LACFCD's planning and operations.

169 Section 2 discusses the development of the LACFCD design storm and the scaling factors'
170 construction. Section 3 summarizes the downscaling and bias-correction steps. The implications
171 of our scaling factors are described in the degree-warming framework in Section 4. Section 5
172 addresses how we communicate the uncertainty in climate simulations to stakeholder groups.
173 Conclusions are presented in Section 6.

# 174 2 Design Storms and Scaling Factors

175

176 The LACFCD oversees the design of urban infrastructure to withstand severe storm activity.
177 That includes gutter sizing, spillway size and spacing, and maintenance hole placement. The
178 design requires an intimate understanding of urban environments, including surface slope,
179 porosity, and the locations of downslope flow convergence during a rainstorm. Each design
180 aspect meets a standard to mitigate a certain level of risk. That risk tolerance is predicated on a
181 return period framework (the inverse of frequency), and standards are designed assuming a
182 certain amount of risk.

183

184 The primary tool for creating these standards is the LACFCD “design storm”. The design storm
185 is the 50-year recurrence of a 24-hour precipitation total. It is created using local rain gauge data

in LA County supplemented by the NOAA Atlas 14 50-year, 24-hour storm product (Bonnin et al., 2006). A minimum of 30 years is required for a rain gauge to be included in the FCD design storm, but some gauges have continuous data for over 100 years. The NOAA Atlas program utilizes RADAR reflectivity and satellite remote sensing data to supplement the areas with sparse *in situ* measurements. When these sources are combined, the Generalized Extreme Value Theorem Type 1 (GEV; Gumbel, 1941) can be employed to calculate the 50-year 24-hour event.

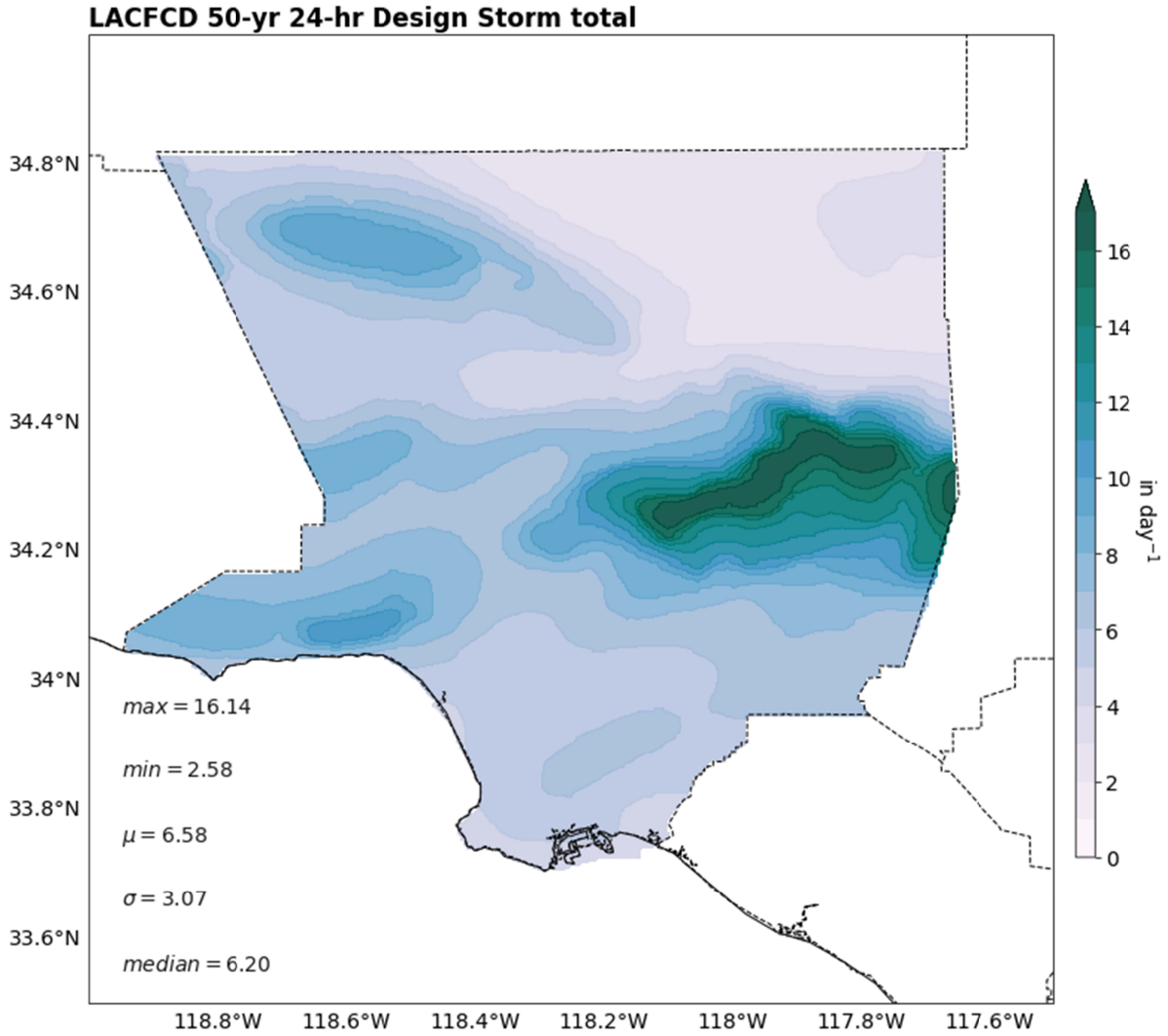


**Figure 1:** Depicts the original LACFCD 50-year, 24-hour design storm. Units are inches/day.

Precipitation in LA County is not homogenous (Fig. 1). Areas with significant topography have greater 50-year 24-hour precipitation values. This is because the precipitation associated with ARs, which deliver almost all extreme precipitation, is enhanced by topography, causing more

intense precipitation at higher elevations, especially on the ocean side of mountains. Significant topography exists in the form of the San Gabriel Mountains in the eastern center of the county, to a lesser extent the Sierra Pelona Mountains in the northwest, and along the western "panhandle" in the Santa Monica Mountains. In the northeast of the county, the climate is mostly arid, which can be inferred from the relatively low values in the 50-year 24-hour storm.

The design storm framework can help establish risk standards based on historical data. It assumes that the statistics that govern the historical period will be similar in the future. However, climate change is not expected to conform to stationarity assumptions. Rather it will establish a new and evolving set of statistics that describe the future period. The LACFCD has operated for over 100 years and thus acquired deep local institutional knowledge that guides its operations. Therefore, developing a climate-aware methodology that will improve their existing framework rather than replace it is prudent. For this task, we create scaling factors that introduce the effects of climate change to their current design storm standards.

To calculate the scaling factors, we find the annual maximum daily precipitation (Rx1day) in each downscaled GCM over each grid space. Then we select two 40-year periods: the first represents the historical era (1981–2020); the second is centered on when the 40-year running mean of global mean surface air temperature (GMT) reaches $\Delta$+3ºC relative to preindustrial conditions (i.e., to 1850–1900 global mean). When this threshold is breached in a particular GCM simulation is specific to that GCMs' climate sensitivity. This definition of the future period is helpful because many aspects of change in the global water cycle, including precipitation scale with temperature changes (Trenberth, 2011). This architecture allows us to remove the uncertainty of choosing an emissions scenario and the model uncertainty within a given emissions scenario and focus on the atmosphere's response to a warmer world.

Using both 40-year periods and the GEV theorem, we calculate two 50-year return period storms. Then we create scaling factors as follows:

$$P_{SF} = \left(\left(\frac{P_{50,24,fut}}{P_{50,24,hist}}\right)\Delta T^{-1}\right) \times 100 \quad (1)$$

where and $P_{50,24,hist}$ and $P_{50,24,fut}$ are the 50-year 24-hour storm from the historical and future periods, and $\Delta T$ is the difference in GMT between the historical and future periods. These calculations produce scaling factors (units = % $^{o}C^{-1}$) that can be applied to the FCD's existing 50-year, 24-hour design storm.

One drawback of this approach is that individual GCMs have a low signal-to-noise ratio for such a low-frequency statistic, primarily due to internal variability. To address this, we pool all eight dynamically-downscaled GCMs to improve robustness in calculating the return period storms, following a similar methodology to Srivastava et al. (2021). By doing so for the historical and future periods separately, the return periods can be calculated from 320 net years, adding confidence to the calculations and improving sampling. This technique is justified by the fact that all historical simulations are driven by bias-corrected GCMs, so that the eight historical simulations all represent the same baseline climate, albeit with differing climate variability; meanwhile, the definition of the future period based on +3ºC warming implies that all eight future simulations represent the same warmer world.

# 3 Model Data

This study utilizes eight dynamically downscaled CMIP6 projections over California at 9-km grid spacing (Rahimi et al., 2023; in preparation). The set of GCMs was selected for downscaling by a multi-step process that prioritizes skillful simulations of California's climate and a balanced representation of projected future changes. To identify the GCMs that most accurately reproduce California's historical climate, CMIP6 models' historical simulations are compared to ERA5 reanalysis data. Each GCM's performance is ranked via metrics that evaluate mean climate conditions, climate variability, frequency, and intensity of extreme conditions over California. In addition, the rankings include the representation of larger-scale circulation features and modes of variability, like the Pacific jet stream and the El Niño Southern Oscillation (ENSO), that play important roles in driving California's climate and variability. The GCMs that perform the best

across this set of metrics are kept as candidates for downscaling. The selected GCMs are summarized in Table 1.

**Table 1: Description of the downscaled simulations' parent GCMs.**

| Country | Modeling Center | Model | Member | Citation |
|---|---|---|---|---|
| USA | National Center for Atmospheric Research | **CESM2** | r11i1p1f1 | Danabasoglu et al., 2020 |
| France | Centre National de Recherches Météorologiques | **CNRM-ESM2-1** | r1i1p1f2 | Séférian et al., 2019 |
| Sweden | Rossby Center, Swedish Meteorological and Hydrological Institute | **EC-EARTH3-VEG** | r1i1p1f1 | Döscher et al., 2022 |
| Sweden | Rossby Center, Swedish Meteorological and Hydrological Institute | **EC-EARTH3** | r1i1p1f1 | Döscher et al., 2022 |
| Canada | Canadian Centre for Climate Modelling and Analysis | **CANESM5** | r1i1p2f1 | Swart et al., 2019 |
| Australia | Commonwealth Scientific and Industrial Research Organisation | **ACCESS-CM2** | r5i1p1f1 | Bi et al., 2020 |
| Germany | Max Planck Institute for Meteorology | **MPI-ESM1-2-LR** | r7i1p1f1 | Mauritsen et al., 2019 |
| United Kingdom | Met Office Hadley Centre | **UKESM1-0-LL** | r1i1p1f1 | Mulcahy et al., 2023 |

Within the best-performing GCMs, most have several individual simulations, known as ensemble members, covering the entire 21st century. All members are subject to the same greenhouse gas forcing, thus simulating very similar changes in mean climate. But, due to the climate system's natural variability, each member captures a different possible sequence of weather events. The range of projections represented across different members contains important information about the uncertainty of future changes and the simulated changes to the statistical likelihood of extreme events. For studies focused on the impacts of extreme precipitation, it is vital to ensure that statistically rare events are sampled in the downscaled ensemble. We note that some institutions that manage GCMs only provide appropriate boundary conditions for a single member, limiting our choice of which ensemble member to downscale.

The future percent change in the 99.99th (approximately the 50-year storm in Los Angeles) percentile daily precipitation in Los Angeles in the selected GCMs, as well as in the broader CMIP6 ensemble, is shown in Figure 2.

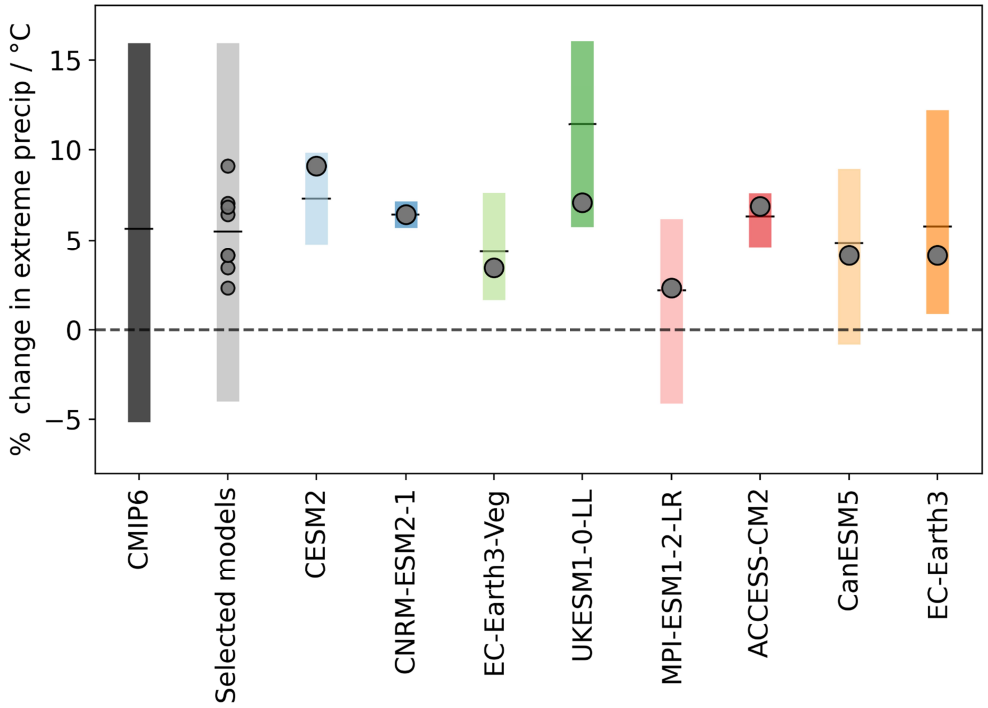


**Figure 2:** The future percent change in the 99.99th percentile precipitation (approximately the 50-year 24-hour storm in Los Angeles, CA; units: % $^{o}C^{-1}$), as represented by the chosen GCMs. The colored bars indicate the spread within each GCM's ensemble suite that we've selected, while the circles represent our downscaled ensemble members. The light grey bar combines all ensemble members from each GCM we downscaled. The dark gray bar represents all ensemble members from the entire CMIP6 ensemble.

While some of our GCM ensembles extend to reach the most extreme precipitation changes seen in the entire CMIP6 ensemble (e.g., UKESM1-0-LL), the ensemble members we downscaled are not extreme in their changes relative to the full CMIP6 suite, and they adequately sample the full CMIP6 ensemble's variability.

The dynamical downscaling was performed using the Weather Research and Forecasting Model version 4.1.3 (Skamarock et al., 2019). Simulations were conducted from 1 August 1980 through 1 September 2100 with future emissions scenarios from the third Shared Socioeconomic Pathway, with a top-of-atmosphere radiative forcing of 7 W $m^{-2}$ by 2100 (SSP3-7.0). Although this study focuses on LA County, the WRF 9-km grid covers all 11 western US states and follows the regional modeling configuration of Rahimi et al., (2022). Before downscaling, the GCMs were bias-corrected following the approach of Bruyère et al. (2014). Please refer to Rahimi et al. (2023a, b; in prep) for a thorough description.

# 4 Extreme precipitation in a warming climate

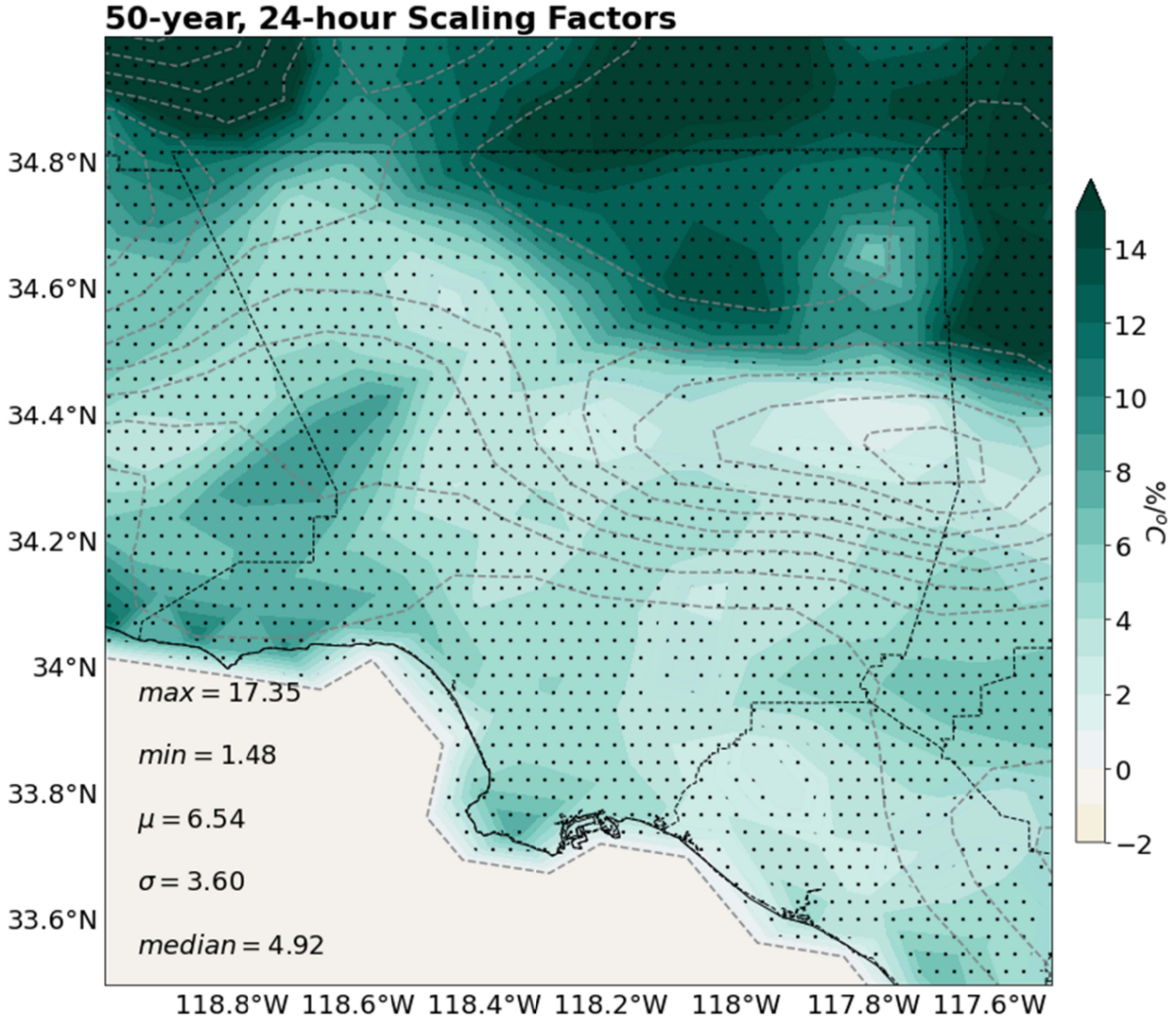

303 **Figure 3:** Shows the scaling factors [derived from % $^{o}C^{-1}$] over Los Angeles County. The thin dashed gray lines are
304 topographic contours at a 200 m increment. The stippled area shows 70% model agreement on the sign of the
305 change signal after bootstrapping the distribution with 1000 samples.

306

307 The final scaling factors are presented in Figure 3. They indicate a general intensification of the
308 design storm, with over 70% of the downscaled simulations plus 1000 bootstrapped supplements
309 agreeing on the sign of that change (stippling). Like the current design storm (Fig. 2), the scaling
310 factors are inconsistent throughout the county, with high values to the north in arid regions and
311 low percentage increases in areas of major orography (gray dashed lines). Theory suggests that
312 extreme precipitation will intensify at ~7% $^{o}C^{-1}$ due to the corresponding increase in saturation
313 specific humidity, predicted by the CC relation. Here, most of the "super-CC" values occur in the
314 northern part of the county (above 14% $C^{-1}$ in large areas). The most substantial percent
315 increases in the northern quarter of the county are also in areas where the 50-year 24-hour storm
316 magnitudes are relatively small, to begin with (See Fig. 2). Yet, the enhanced values in the
317 northeast of the county are consistent with studies that have found disproportionately large
318 increases in lee-side precipitation under climate change (Siler & Roe, 2014). The average scaling
319 factor in the county is slightly less than CC predicts ( 6.5% $^{o}C^{-1}$) but is still within a reasonable
320 range (Zhang et al., 2013). The range of projected increases in the 50-year 24-hour storm within
321 the county is 1.48% $^{o}C^{-1}$ and 17.35% $^{o}C^{-1}$ (Fig. 3).

322 The CC relation is based on thermodynamic effects only. However, as climate evolves, the
323 atmospheric circulation will shift too, resulting in non-uniform changes in extreme precipitation
324 (Pfahl et al., 2017), as depicted in Fig. 3. Furthermore, in contrast to the high desert (i.e., NE of
325 the county) where the signal is clear (i.e., stippled), other parts of the county do not meet the
326 same criteria for a significant signal. This could be because the GCMs themselves have differing
327 representations of, for example, ENSO—a major driver of the natural variability—leading to
328 different change signals.

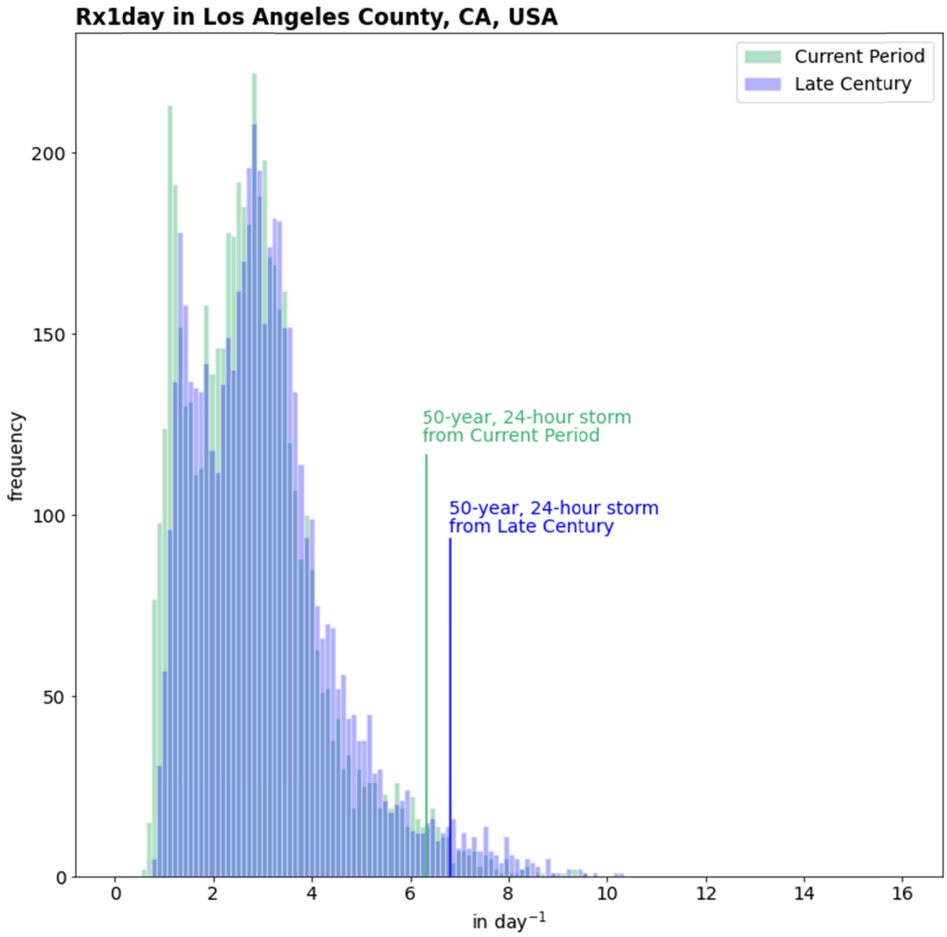


**Figure 4:** Histograms of the spatial variation of extreme precipitation in the current period (1980–2020; green) and a future period (2060–2100; blue) using GCM ensemble mean 40 year of Rx1day over all grid cells in Los Angeles County.

Figure 4 contrasts the frequency distributions of 50-year 24-hour precipitation using all grid points in Los Angeles County. Each location has a 40-year annual maximum series in the current and end-of-century periods. Although there are varying rates of warming between models, the late-century histogram portrays a general shift to more intense precipitation, consistent with theory (Trenberth, 2011). This is apparent in the decreased peak and longer tail, compared to the historical distribution, consistent with previous work evaluating sub-daily precipitation extremes over California (Moustakis et al., 2021).

Instead of predicted end-of-century changes, we may express changes under various warming levels, as derived in the previous section. To apply the scaling factors in Figure 3, they are

345 bilinearly interpolated to the LACFCD's native GIS grid that hosts the current design storm
346 (Figure 1). The current design storm is adjusted using the following equation:

$$MF = \left(\frac{(P_{SF} + 100)}{100}\right)^{\Delta T} \quad (2)$$

347 where $P_{SF}$ is the precipitation scaling factor (Fig. 3), and MF is the resulting multiplicative
348 factor, again following (Martel et al., 2021).
349
350 Figure 5 provides a detailed illustration of the effects of climate change at three relevant
351 warming horizons: 2º, 3º, and 4º of global warming relative to a preindustrial average
352 temperature (1850–1900 mean). Averaged over LA County, there is an increase of 0.44, 0.82,
353 and 1.22 in/day under 2º, 3º, and 4º warming, respectively. The Transverse Ranges, in particular
354 the Santa Monica and San Gabriel Mountains, experience the greatest increases. This largely
355 reflects the greater historical values, although it is noteworthy that the Santa Monica mountains
356 experience the greatest increases, despite being historically drier than the San Gabriels. For
357 example, averaged over the Santa Monica Mountains (i.e., in the southwest of the county along
358 the coast), the design storm increases from 9 in/day historically to 10, 10.9, and 12.0 in/day
359 under 2º, 3º, and 4º warming, respectively; meanwhile, averaged over the San Gabriels (i.e., in
360 the eastern center of the county), there is an increase from around 17 in/day historically to 17.9,
361 18.7, and 19.6 in/day under 2º, 3º, and 4º warming.
362

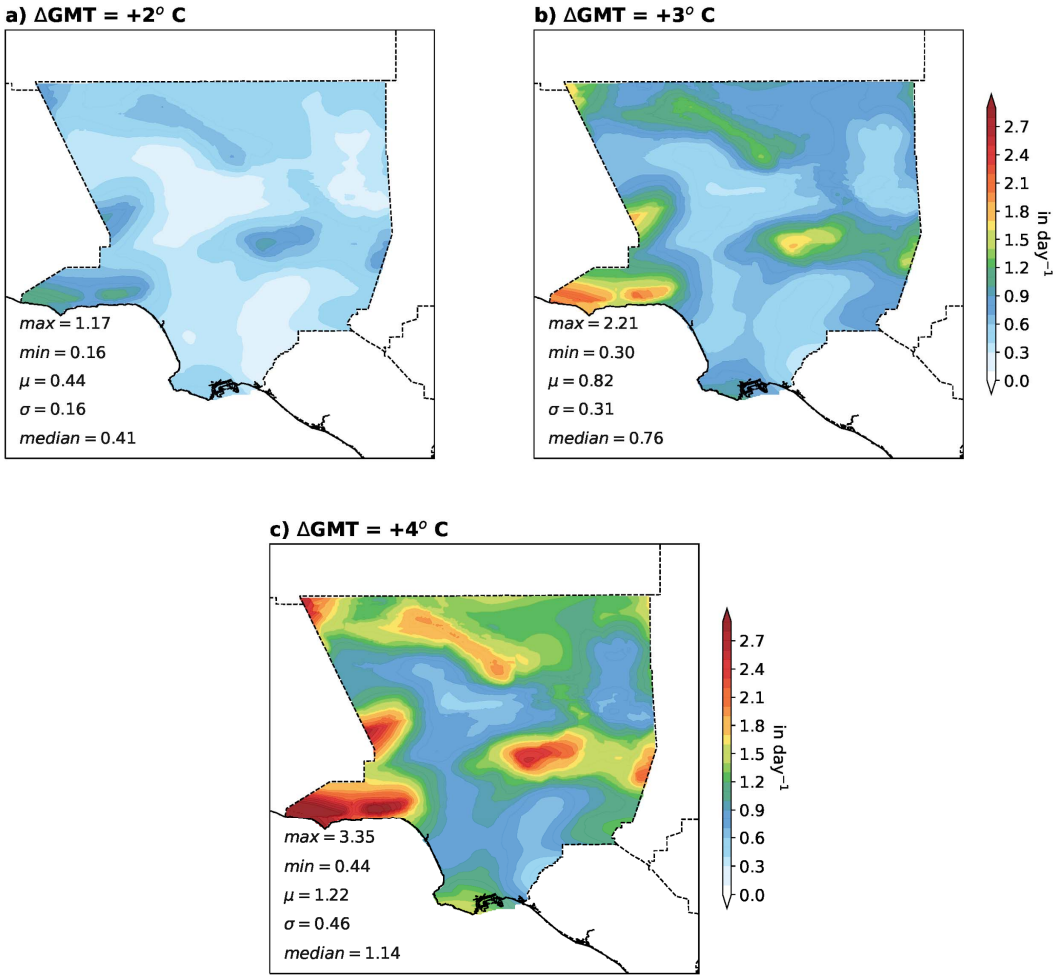


**Figure 5:** Changes in the 50-year 24-hour storm over LA County on the LACFCD's original grid after scaling factors have been applied for (a) a 2º, (b) a 3º, and (c) a 4º world [in day$^{-1}$]. Statistics of the changes in the county are shown in the lower right corner of each panel.

These future design storm possibilities are conditioned on the given global warming levels to align with benchmarks emerging from the national and international climate policy conversation. As socio-economic and political conditions evolve, managers can update their estimations on which global warming level is likely to be reached within their planning horizon. For example, there is a consensus that 2˚ of global warming is almost inevitable sometime in the mid-21st Century, while 3˚ is likely by the end of the century (IPCC, 2021). Therefore, applying our scaling factors, by mid-century, design storm increases exceeding 0.5 inches over mountainous areas are almost inevitable (+2º C warming), and by the end of the century, increases of 3 inches are possible in the 4º scenario.

The LACFCD is using the warming-dependent projections to force a GIS-based runoff model that includes the myriad land surface information of Los Angeles County (i.e., permeability, land cover, and infrastructure). Thus, the expected level of flooding may be predicted for the design storm under a prescribed level of global warming, and they can explore the implications of these projections in planning exercises.

# 5 Communicating Uncertainty to Stakeholders

In this study, we have stressed the importance of accurately conveying the sources of uncertainty to stakeholders when guiding climate resilience planning. We will address three primary sources of uncertainty in regional climate simulations (discussed in, e.g., Hawkins & Sutton, 2009) in this section. These provide a framework for communicating the challenges and opportunities in utilizing regional climate projections for climate adaptation and mitigation. These three sources of uncertainty and how we approach them are schematically shown in Figure 6.

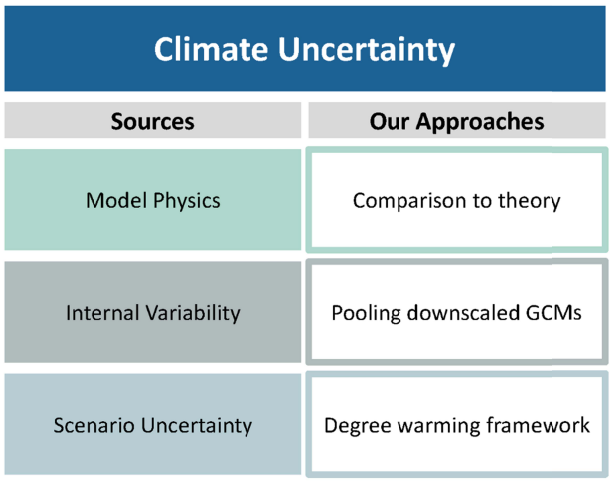


**Figure 6:** Describes (left) the sources of regional climate uncertainty as outlined by Hawkins and Sutton (2009) and (right) our mechanisms for addressing them to the stakeholders.

First, model physics refers to the choices representing the various physical processes in a GCM or RCM (e.g., radiation, cloud processes, convection, etc.). Sub-grid scale processes require

physical parameterizations that represent the relevant processes without explicitly resolving them. Parameterizations are essential in modeling, but each introduces differences in how models behave. These physics packages can collectively interact and alter an RCM simulation's results. The uncertainty arising from variations in model results can be expressed as just the spread across the model outcome for the same climate forcing. In addition, the uncertainty can be assessed by comparing the models' collective performance to known climate physics. In our case, CC theory suggests that daily extreme precipitation should increase by approximately ~7% $^{o}C^{-1}$. Comparisons of the models' projections (6.5% $^{o}C^{-1}$ averaged over the county) to theory imply that the models are collectively performing approximately as expected, giving confidence in our main results (e.g. Figure 3) despite the inter-model variation.

Second, internal variability derives from the natural processes that occur on different timescales in the Earth system. Hawkins and Sutton (2009) show that the influence of internal variability on GMT evolution is significant in the near term but decreases in importance as the century progresses. Because of internal variability, it is not meaningful to use a single climate model simulation to guide adaptation. Dong et al. (2021) use 318 climate simulations to quantify uncertainty due to internal variability. Because individual simulations have different phasing of variability, any two climate-model realizations may differ significantly in their representation of precipitation at the regional scale. To address this source of uncertainty with the stakeholders, we pool all 8 GCMs' dynamically downscaled simulations together, maximizing the sample size. This is analogous to utilizing an ensemble from a single GCM, given that all GCMs' historical simulations are bias-corrected prior to downscaling. By maximizing our sample size, internal variability effects can be better constrained and understood, and we can more confidently advise the stakeholders.

Finally, the choice of emissions scenario is a source of deep uncertainty. The degree-warming framework takes advantage of the fact that precipitation responds more directly to temperature than to emissions. Therefore, the question can shift from "Which emissions scenario should we choose?" to "When is a given global warming level likely to occur?" This eliminates the economic and geopolitical assumptions that are highly challenging to define, particularly for stakeholders who may lack expertise in these topics. Then as socioeconomic and political

conditions evolve, stormwater managers can employ adaptive planning strategies that update over time, leading to self-correcting resilience.

# 6 Conclusions

By assessing the state-of-the-art GCMs from CMIP6, we have identified a cohort of models that better capture the large-scale atmospheric conditions associated with extreme precipitation in LA County historically. We downscaled the 21st-Century projections from these top-performing simulations over the western U.S. with a regional climate model. These local projections have allowed us to examine the changes to a design storm over LA County under a range of future scenarios. These future design storm possibilities are conditioned on global warming levels of 2˚, 3˚, and 4˚ from pre-industrial times to align with benchmarks that have emerged from the national and international climate policy conversation. Averaged over LA County, there is an increase of 0.44, 0.82, and 1.22 in/day under 2º, 3º, and 4º warming, respectively, with larger increases over the mountainous regions. The 2˚ scenario will inevitably be experienced at some point in the mid-century (Kriegler et al., 2018), regardless of emissions trajectory. Other emissions scenarios result in greater warming levels being reached by the end of this century. By anticipating the associated local impacts, the LACFCD can adaptively manage its planning as the uncertainty in timing is reduced (i.e., based on the emissions trajectory the world ends up following).

By focusing on the 50-year, 24-hour design storm, we provide a standard reference for stormwater engineers. Each return period (e.g., a storm that occurs on average once every 50 years) and duration (the precipitation totals accumulated over, e.g., a full 24 hours) are tied to stormwater planning policies. Stormwater engineers in the LACFCD are accustomed to relating these to each other through standard statistical distributions described in their hydrology manual. By providing a 50-year, 24-hour storm for future conditions at various warming levels, the climate scientists in our collaboration enable the LACFCD planners to simulate how the surface hydrology would respond to a complete set of design storms at a range of durations and return periods.

# Acknowledgements

This research was supported by the Los Angeles County - Dept of Public Works Award Number 20195156. The authors would like to acknowledge our partners, the engineering team at the Los Angeles County Flood Control District, for numerous constructive conversations.


# Data Availability Statement

All downscaled data, including the daily post-processed datastream (Tier 3) used here, are located in the following open-data bucket on Amazon S3: s3://wrf-cmip6-noversioning/ at https://registry.opendata.aws/wrf-cmip6/. These data are completely open and free to the public. We have also developed a technical access and usage document that details these three data tiers which can be found at https://dept.atmos.ucla.edu/sites/default/files/alexhall/files/aws_tiers_dirstructure_nov22.pdf. These data are most easily downloaded when using Amazon Web Service's (AWS') Command Line Interface (CLI) or with the command 'wget'. An example is presented in the technical access and usage document. The specific GCMs used here are eight of the 9-km, bias-corrected GCMs described in Table 1.

# References


Alexander, L. V., Zhang, X., Peterson, T. C., Caesar, J., Gleason, B., Klein Tank, A. M. G., et al. (2006). Global observed changes in daily climate extremes of temperature and precipitation. *Journal of Geophysical Research: Atmospheres*, *111*(D5). https://doi.org/10.1029/2005JD006290

Arnbjerg-Nielsen, K., Willems, P., Olsson, J., Beecham, S., Pathirana, A., Bülow Gregersen, I., et al. (2013). Impacts of climate change on rainfall extremes and urban drainage systems: a review. *Water Science and Technology*, *68*(1), 16–28. https://doi.org/10.2166/wst.2013.251

Arnbjerg-Nielsen, Karsten. (2012). Quantification of climate change effects on extreme precipitation used for high resolution hydrologic design. *Urban Water Journal*, *9*(2), 57–65. https://doi.org/10.1080/1573062X.2011.630091

Barnett, T. P., Pierce, D. W., Hidalgo, H. G., Bonfils, C., Santer, B. D., Das, T., et al. (2008). Human-Induced Changes in the Hydrology of the Western United States. *Science*, *319*(5866), 1080–1083. https://doi.org/10.1126/science.1152538

Bass, B., Goldenson, N., Rahimi, S., & Hall, A. (2023). Aridification of Colorado River Basin's Snowpack Regions Has Driven Water Losses Despite Ameliorating Effects of Vegetation. *Water Resources Research*, *59*(7), e2022WR033454. https://doi.org/10.1029/2022WR033454

Berg, N., & Hall, A. (2015). Increased Interannual Precipitation Extremes over California under Climate Change. *Journal of Climate*, *28*(16), 6324–6334. https://doi.org/10.1175/JCLI-D-14-00624.1

Bi, D., Dix, M., Marsland, S., O'Farrell, S., Sullivan, A., Bodman, R., et al. (2020). Configuration and spin-up of ACCESS-CM2, the new generation Australian Community Climate and Earth System Simulator Coupled Model. *Journal of Southern Hemisphere Earth Systems Science*, *70*(1), 225–251. https://doi.org/10.1071/ES19040

Bonnin, G., Martin, D., Lin, B., & Parzybok, T. (2006). Precipitation-frequency atlas of the United States. *NOAA*, *1*, 1–17. https://doi.org/10.1166/Sl.2008.003

Bruyère, C. L., Done, J. M., Holland, G. J., & Fredrick, S. (2014). Bias corrections of global models for regional climate simulations of high-impact weather. *Climate Dynamics*, *43*(7), 1847–1856. https://doi.org/10.1007/s00382-013-2011-6

505 Chen, X., Leung, L. R., Gao, Y., Liu, Y., & Wigmosta, M. (2023). Sharpening of cold-season storms over the
506 western United States. *Nature Climate Change*, 1–7. https://doi.org/10.1038/s41558-022-01578-0
507 Cheng, L., & AghaKouchak, A. (2014). Nonstationary Precipitation Intensity-Duration-Frequency Curves for
508 Infrastructure Design in a Changing Climate. *Scientific Reports*, *4*(1), 7093.
509 https://doi.org/10.1038/srep07093
510 Cook, L. M., Anderson, C. J., & Samaras, C. (2017). Framework for Incorporating Downscaled Climate Output into
511 Existing Engineering Methods: Application to Precipitation Frequency Curves. *Journal of Infrastructure*
512 *Systems*, *23*(4), 04017027. https://doi.org/10.1061/(ASCE)IS.1943-555X.0000382
513 Corringham, T. W., McCarthy, J., Shulgina, T., Gershunov, A., Cayan, D. R., & Ralph, F. M. (2022). Climate
514 change contributions to future atmospheric river flood damages in the western United States. *Scientific*
515 *Reports*, *12*(1), 13747. https://doi.org/10.1038/s41598-022-15474-2
516 Danabasoglu, G., Lamarque, J.-F., Bacmeister, J., Bailey, D. A., DuVivier, A. K., Edwards, J., et al. (2020). The
517 Community Earth System Model Version 2 (CESM2). *Journal of Advances in Modeling Earth Systems*,
518 *12*(2), e2019MS001916. https://doi.org/10.1029/2019MS001916
519 Das, T., Dettinger, M. D., Cayan, D. R., & Hidalgo, H. G. (2011). Potential increase in floods in California's Sierra
520 Nevada under future climate projections. *Climatic Change*, *109*(1), 71–94. https://doi.org/10.1007/s10584-
521 011-0298-z
522 Das, T., Maurer, E. P., Pierce, D. W., Dettinger, M. D., & Cayan, D. R. (2013). Increases in flood magnitudes in
523 California under warming climates. *Journal of Hydrology*, *501*, 101–110.
524 https://doi.org/10.1016/j.jhydrol.2013.07.042
525 Dettinger, M. (2011). Climate Change, Atmospheric Rivers, and Floods in California – A Multimodel Analysis of
526 Storm Frequency and Magnitude Changes1. *JAWRA Journal of the American Water Resources*
527 *Association*, *47*(3), 514–523. https://doi.org/10.1111/j.1752-1688.2011.00546.x
528 Dettinger, M. D. (2013). Atmospheric Rivers as Drought Busters on the U.S. West Coast. *Journal of*
529 *Hydrometeorology*, *14*(6), 1721–1732. https://doi.org/10.1175/JHM-D-13-02.1
530 Dong, L., Leung, L. R., Song, F., & Lu, J. (2021). Uncertainty in El Niño-like warming and California precipitation
531 changes linked by the Interdecadal Pacific Oscillation. *Nature Communications*, *12*(1), 6484.
532 https://doi.org/10.1038/s41467-021-26797-5

Döscher, R., Acosta, M., Alessandri, A., Anthoni, P., Arsouze, T., Bergman, T., et al. (2022). The EC-Earth3 Earth system model for the Coupled Model Intercomparison Project 6. *Geoscientific Model Development*, *15*(7), 2973–3020. https://doi.org/10.5194/gmd-15-2973-2022

Fadhel, S., Rico-Ramirez, M. A., & Han, D. (2017). Uncertainty of Intensity–Duration–Frequency (IDF) curves due to varied climate baseline periods. *Journal of Hydrology*, *547*, 600–612. https://doi.org/10.1016/j.jhydrol.2017.02.013

Fischer, E. M., & Knutti, R. (2015). Anthropogenic contribution to global occurrence of heavy-precipitation and high-temperature extremes. *Nature Climate Change*, *5*(6), 560–564. https://doi.org/10.1038/nclimate2617

Fowler, H. J., Wasko, C., & Prein, A. F. (2021). Intensification of short-duration rainfall extremes and implications for flood risk: current state of the art and future directions. *Philosophical Transactions of the Royal Society A*. https://doi.org/10.1098/rsta.2019.0541

Gumbel, E. J. (1941). The Return Period of Flood Flows. *The Annals of Mathematical Statistics*, *12*(2), 163–190. https://doi.org/10.1214/aoms/1177731747

Hall, A., Berg, N., & Reich, K. (2018). *Los Angeles Summary Report* (California's Fourth Climate Change Assessment No. SUM-CCCA4-2018-007). University of California Los Angeles.

Harris, S. M., & Carvalho, L. M. V. (2018). Characteristics of southern California atmospheric rivers. *Theoretical and Applied Climatology*, *132*(3), 965–981. https://doi.org/10.1007/s00704-017-2138-1

Hawkins, E., & Sutton, R. (2009). The Potential to Narrow Uncertainty in Regional Climate Predictions. *Bulletin of the American Meteorological Society*, *90*(8), 1095–1108. https://doi.org/10.1175/2009BAMS2607.1

Hodgkins, G. A., Dudley, R. W., Archfield, S. A., & Renard, B. (2019). Effects of climate, regulation, and urbanization on historical flood trends in the United States. *Journal of Hydrology*, *573*, 697–709. https://doi.org/10.1016/j.jhydrol.2019.03.102

Huang, X., & Swain, D. L. (2022). Climate change is increasing the risk of a California megaflood. *Science Advances*, *8*(32), eabq0995. https://doi.org/10.1126/sciadv.abq0995

IPCC. (2021). Summmary for Policy Makers. In *Claime Change 2021: The Physical Science Basis. Contribution of Working Group I to the Sixth Assessment Report of the Intergovernmental Panel on Climate Change* (pp. 3–32). Cambridge, United Kingdom and New York, NY, USA: Cambridge University Press. Retrieved from 10.1017/9781009157896.001

561 Kirchmeier-Young, M. C., & Zhang, X. (2020). Human influence has intensified extreme precipitation in North
562 America. *Proceedings of the National Academy of Sciences*, *117*(24), 13308–13313.
563 https://doi.org/10.1073/pnas.1921628117
564 Kriegler, E., Luderer, G., Bauer, N., Baumstark, L., Fujimori, S., Popp, A., et al. (2018). Pathways limiting warming
565 to 1.5°C: a tale of turning around in no time? *Philosophical Transactions of the Royal Society A:*
566 *Mathematical, Physical and Engineering Sciences*, *376*(2119), 20160457.
567 https://doi.org/10.1098/rsta.2016.0457
568 Kunkel, K. E. (2003). North American Trends in Extreme Precipitation. *Natural Hazards*, *29*(2), 291–305.
569 https://doi.org/10.1023/A:1023694115864
570 Madakumbura, G. D., Thackeray, C. W., Norris, J., Goldenson, N., & Hall, A. (2021). Anthropogenic influence on
571 extreme precipitation over global land areas seen in multiple observational datasets. *Nature*
572 *Communications*, *12*(1), 3944. https://doi.org/10.1038/s41467-021-24262-x
573 Mailhot, A., & Duchesne, S. (2010). Design Criteria of Urban Drainage Infrastructures under Climate Change.
574 *Journal of Water Resources Planning and Management*, *136*(2), 201–208.
575 https://doi.org/10.1061/(ASCE)WR.1943-5452.0000023
576 Martel, J.-L., Brissette, F. P., Lucas-Picher, P., Troin, M., & Arsenault, R. (2021). Climate Change and Rainfall
577 Intensity–Duration–Frequency Curves: Overview of Science and Guidelines for Adaptation. *Journal of*
578 *Hydrologic Engineering*, *26*(10), 03121001. https://doi.org/10.1061/(ASCE)HE.1943-5584.0002122
579 Mauritsen, T., Bader, J., Becker, T., Behrens, J., Bittner, M., Brokopf, R., et al. (2019). Developments in the MPI-M
580 Earth System Model version 1.2 (MPI-ESM1.2) and Its Response to Increasing CO2. *Journal of Advances*
581 *in Modeling Earth Systems*, *11*(4), 998–1038. https://doi.org/10.1029/2018MS001400
582 Min, S.-K., Zhang, X., Zwiers, F. W., & Hegerl, G. C. (2011). Human contribution to more-intense precipitation
583 extremes. *Nature*, *470*(7334), 378–381. https://doi.org/10.1038/nature09763
584 Monier, E., & Gao, X. (2015). Climate change impacts on extreme events in the United States: an uncertainty
585 analysis. *Climatic Change*, *131*(1), 67–81. https://doi.org/10.1007/s10584-013-1048-1
586 Moustakis, Y., Papalexiou, S. M., Onof, C. J., & Paschalis, A. (2021). Seasonality, Intensity, and Duration of
587 Rainfall Extremes Change in a Warmer Climate. *Earth's Future*, *9*(3), e2020EF001824.
588 https://doi.org/10.1029/2020EF001824

589 Mulcahy, J. P., Jones, C. G., Rumbold, S. T., Kuhlbrodt, T., Dittus, A. J., Blockley, E. W., et al. (2023).
590 UKESM1.1: development and evaluation of an updated configuration of the UK Earth System Model.
591 *Geoscientific Model Development*, *16*(6), 1569–1600. https://doi.org/10.5194/gmd-16-1569-2023
592 O'Gorman, P. A. (2015). Precipitation Extremes Under Climate Change. *Current Climate Change Reports*, *1*(2),
593 49–59. https://doi.org/10.1007/s40641-015-0009-3
594 Pendergrass, A. G. (2018). What precipitation is extreme? *Science*, *360*(6393), 1072–1073.
595 https://doi.org/10.1126/science.aat1871
596 Pfahl, S., O'Gorman, P. A., & Fischer, E. M. (2017). Understanding the regional pattern of projected future changes
597 in extreme precipitation. *Nature Climate Change*, *7*(6), 423–427. https://doi.org/10.1038/nclimate3287
598 Ragno, E., AghaKouchak, A., Love, C. A., Cheng, L., Vahedifard, F., & Lima, C. H. R. (2018). Quantifying
599 Changes in Future Intensity-Duration-Frequency Curves Using Multimodel Ensemble Simulations. *Water*
600 *Resources Research*, *54*(3), 1751–1764. https://doi.org/10.1002/2017WR021975
601 Rahimi, S., Krantz, W., Lin, Y.-H., Bass, B., Goldenson, N., Hall, A., et al. (2022). Evaluation of a Reanalysis-
602 Driven Configuration of WRF4 Over the Western United States From 1980 to 2020. *Journal of*
603 *Geophysical Research: Atmospheres*, *127*(4), e2021JD035699. https://doi.org/10.1029/2021JD035699
604 Ralph, F. M., Neiman, P. J., Wick, G. A., Gutman, S. I., Dettinger, M. D., Cayan, D. R., & White, A. B. (2006).
605 Flooding on California's Russian River: Role of atmospheric rivers. *Geophysical Research Letters*, *33*(13).
606 https://doi.org/10.1029/2006GL026689
607 Sanders, B. F., Schubert, J. E., Kahl, D. T., Mach, K. J., Brady, D., AghaKouchak, A., et al. (2022). Large and
608 inequitable flood risks in Los Angeles, California. *Nature Sustainability*, 1–11.
609 https://doi.org/10.1038/s41893-022-00977-7
610 Séférian, R., Nabat, P., Michou, M., Saint-Martin, D., Voldoire, A., Colin, J., et al. (2019). Evaluation of CNRM
611 Earth System Model, CNRM-ESM2-1: Role of Earth System Processes in Present-Day and Future Climate.
612 *Journal of Advances in Modeling Earth Systems*, *11*(12), 4182–4227.
613 https://doi.org/10.1029/2019MS001791
614 Sharma, A., Wasko, C., & Lettenmaier, D. P. (2018). If Precipitation Extremes Are Increasing, Why Aren't Floods?
615 *Water Resources Research*, *54*(11), 8545–8551. https://doi.org/10.1029/2018WR023749

Shepherd, T. G., Boyd, E., Calel, R. A., Chapman, S. C., Dessai, S., Dima-West, I. M., et al. (2018). Storylines: an alternative approach to representing uncertainty in physical aspects of climate change. *Climatic Change*, *151*(3), 555–571. https://doi.org/10.1007/s10584-018-2317-9

Siler, N., & Roe, G. (2014). How will orographic precipitation respond to surface warming? An idealized thermodynamic perspective. *Geophysical Research Letters*, *41*(7), 2606–2613. https://doi.org/10.1002/2013GL059095

Srivastav, R. K., Schardong, A., & Simonovic, S. P. (2014). Equidistance Quantile Matching Method for Updating IDFCurves under Climate Change. *Water Resources Management*, *28*(9), 2539–2562. https://doi.org/10.1007/s11269-014-0626-y

Srivastava, A. K., Grotjahn, R., Ullrich, P. A., & Sadegh, M. (2021). Pooling Data Improves Multimodel IDF Estimates over Median-Based IDF Estimates: Analysis over the Susquehanna and Florida. *Journal of Hydrometeorology*, *22*(4), 971–995. https://doi.org/10.1175/JHM-D-20-0180.1

Sutton, R. T. (2019). Climate Science Needs to Take Risk Assessment Much More Seriously. *Bulletin of the American Meteorological Society*, *100*(9), 1637–1642. https://doi.org/10.1175/BAMS-D-18-0280.1

Swain, D. L., Langenbrunner, B., Neelin, J. D., & Hall, A. (2018). Increasing precipitation volatility in twenty-first-century California. *Nature Climate Change*, *8*(5), 427–433. https://doi.org/10.1038/s41558-018-0140-y

Swart, N. C., Cole, J. N. S., Kharin, V. V., Lazare, M., Scinocca, J. F., Gillett, N. P., et al. (2019). The Canadian Earth System Model version 5 (CanESM5.0.3). *Geoscientific Model Development*, *12*(11), 4823–4873. https://doi.org/10.5194/gmd-12-4823-2019

Trenberth, K. (2011). Changes in Precipitation with Climate Change. *Climate Research*, *47*(1), 123–38.

Wasko, C., & Nathan, R. (2019). Influence of changes in rainfall and soil moisture on trends in flooding. *Journal of Hydrology*, *575*, 432–441. https://doi.org/10.1016/j.jhydrol.2019.05.054

Wasko, C., Westra, S., Nathan, R., Orr, H. G., Villarini, G., Herrera, R. V., & Fowler, H. J. (2021). Incorporating climate change in flood estimation guidance. *Philosophical Transactions of the Royal Society A*. https://doi.org/10.1098/rsta.2019.0548

Westra, S., Alexander, L. V., & Zwiers, F. W. (2013). Global Increasing Trends in Annual Maximum Daily Precipitation. *Journal of Climate*, *26*(11), 3904–3918. https://doi.org/10.1175/JCLI-D-12-00502.1

643 Yan, L., Xiong, L., Jiang, C., Zhang, M., Wang, D., & Xu, C.-Y. (2021). Updating intensity–duration–frequency
644 curves for urban infrastructure design under a changing environment. *Wiley Interdisciplinary Reviews:*
645 *Water*, *8*(3), e1519. https://doi.org/10.1002/wat2.1519
646 Yilmaz, A. G., Hossain, I., & Perera, B. J. C. (2014). Effect of climate change and variability on extreme rainfall
647 intensity–frequency–duration relationships: a case study of Melbourne. *Hydrology and Earth System*
648 *Sciences*, *18*(10), 4065–4076. https://doi.org/10.5194/hess-18-4065-2014
649 Zhang, X., Wan, H., Zwiers, F. W., Hegerl, G. C., & Min, S.-K. (2013). Attributing intensification of precipitation
650 extremes to human influence. *Geophysical Research Letters*, *40*(19), 5252–5257.
651 https://doi.org/10.1002/grl.51010
652